

# Characterisation of the charge sharing in pixellated Si detectors with single-photon processing readout

Börje Norlin<sup>a,\*</sup>, Christer Fröjdh<sup>a</sup>, Hans-Erik Nilsson<sup>a</sup>, Heinz Graafsma<sup>b</sup>,  
Vedran Vonk<sup>b</sup>, Cyril Ponchut<sup>b</sup>

<sup>a</sup>Department of Information Technology and Media, Mid-Sweden University, SE-85170 Sundsvall, Sweden

<sup>b</sup>Experimental Division, ESRF, BP2200 Avenue des Martyrs, 38043 Grenoble, Cedex, France

Available online 17 February 2006

## Abstract

Pixellated silicon detectors with a thickness of 300 and 700  $\mu\text{m}$  bonded to the MEDIPIX2 readout chip have been characterised using a monoenergetic microbeam at the ESRF. The spectral response when a  $10 \times 10 \mu\text{m}^2$  wide 40 keV beam is centred on a single pixel is achieved. When the beam is scanned over the pixel, the charge sharing will increase when the beam approaches the border of the pixel.

The experimental results have been verified by charge transport simulations and X-ray scattering simulations. Agreement between measurements and simulations can be achieved if a wider beam is assumed in the simulations. Widening of the absorption profile can to a large extent be explained by backscattering of lower-energy photons by the tin/led bump bounds below the detector. Widening of the detected beam is also an effect of angular alignment problems, especially on the 700  $\mu\text{m}$  detector. Since the angle between the depth and a half-pixel is only  $2.2^\circ$ , alignment of thick pixellated silicon detectors will be a problem to consider when designing X-ray imaging setups.

© 2006 Published by Elsevier B.V.

PACS: 07.07.Df; 07.85.-m; 07.85.Nc; 07.85.Qe; 78.70.Ck; 78.70.Dm; 87.57.-s; 87.59.-e; 87.62.+n

Keywords: Charge sharing; X-ray; Medipix; Pixel detector; Monte Carlo simulation; Synchrotron radiation

## 1. Background and experimental conditions

Pixel detectors using single-photon processing readout are interesting because of low-noise operation and their ability to record the energy of each individual photon [1]. One such readout chip is the MEDIPIX2 chip [2] with a pixel size of  $55 \times 55 \mu\text{m}^2$ . It has, however, been observed that significant charge sharing occurs for most detectors with small pixels [3]. The charge sharing strongly affects the energy information in the image. In this experiment we have been using a MEDIPIX2 chip bonded to silicon detectors with different thickness and measured the response when exposed with a narrow monoenergetic X-ray beam.

The measurements were performed at the ESRF using a monoenergetic beam with photon energy of 40 keV. A set

of motor driven slits, located about 10 cm from the detector were used to adjust the beam width to  $10 \times 10 \mu\text{m}^2$ . The slits were made of 2 mm thick tungsten with a slight angle. A second pair of slits were mounted closer to the detector to suppress scattered radiation from the first pair. A MEDIPIX detector was mounted on an XY-translation stage to move between the pixels and a rotation stage to align the detector perpendicular to the beam. During the calibration phase the 300  $\mu\text{m}$  silicon detector was used as a reference. After calibration, data were taken with this detector and a 700  $\mu\text{m}$  thick detector. The beam width was verified both by measuring the flux of X-ray photons through the slit and by scanning the beam across a pixel. Almost no scattered photons were visible in the neighbouring pixels. The final beam intensity was around 65,000 photons/s. The applied bias was 100 V for the 300  $\mu\text{m}$  detector and 250 V for the 700  $\mu\text{m}$  detector. The readout was controlled by MUROS2 and Medisoft4 [4].

\*Corresponding author. Tel.: +46 60 148594; fax: +46 60 148456.

E-mail address: [borje.norlin@miiun.se](mailto:borje.norlin@miiun.se) (B. Norlin).

2. Measurements

Spectra for a centred beam for both 300 (Fig. 1) and 700  $\mu\text{m}$  (Fig. 2) thick detectors were achieved by automatic low threshold scans. The raw data from each threshold scan is a cumulative spectrum which is then differentiated. In the differential spectrum a distinct 40 keV peak appears. The width and the position of the peak are discussed in chapter 3.

A direct observation is that lower energies are present in the spectra, although the beam is monochrome and the charge sharing is strongly suppressed by the narrow centred beam. Simulations using MCNP [5] show that this presence of low-energy counts is due to X-ray fluorescence from the bump-bonding [6]. The slope in the cumulative spectrum can be reproduced if indium or tin/lead is present below the detector in the MCNP model, as shown in Fig. 3. The two Medipix chips in the measurements used tin/lead for bump bonding of the detector. The  $K\alpha$  energies for tin and lead are 25 and 75 keV, the 12 keV peak originates from the Pb L-shell. These energies are not expected to be

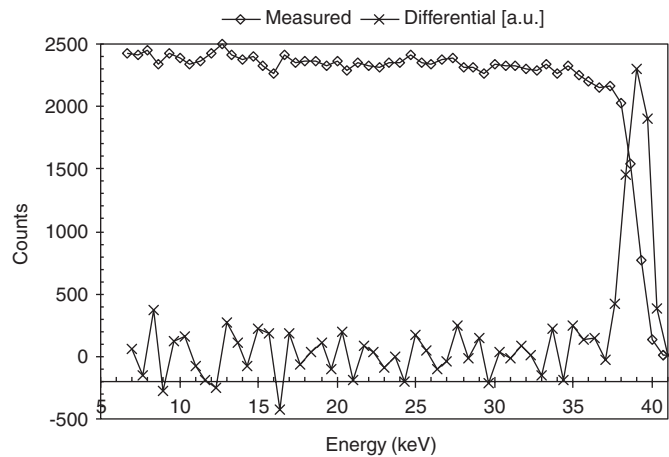


Fig. 1. Measured cumulative spectrum and differential spectrum for a 300  $\mu\text{m}$  thick silicon detector with the beam centred on a pixel.

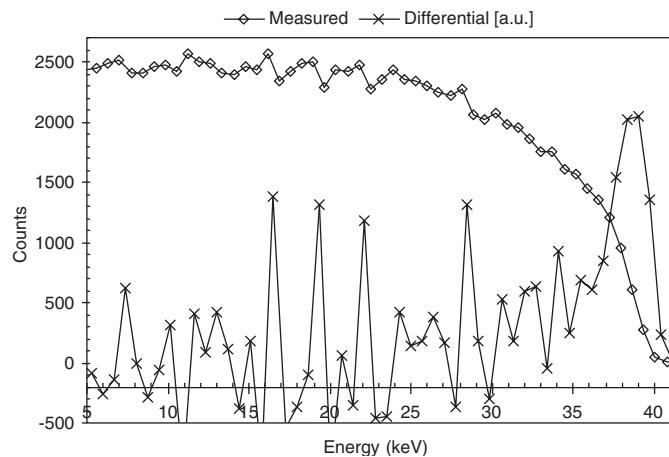


Fig. 2. Measured cumulative spectrum and differential spectrum for a 700  $\mu\text{m}$  thick silicon detector with the beam centred on a pixel.

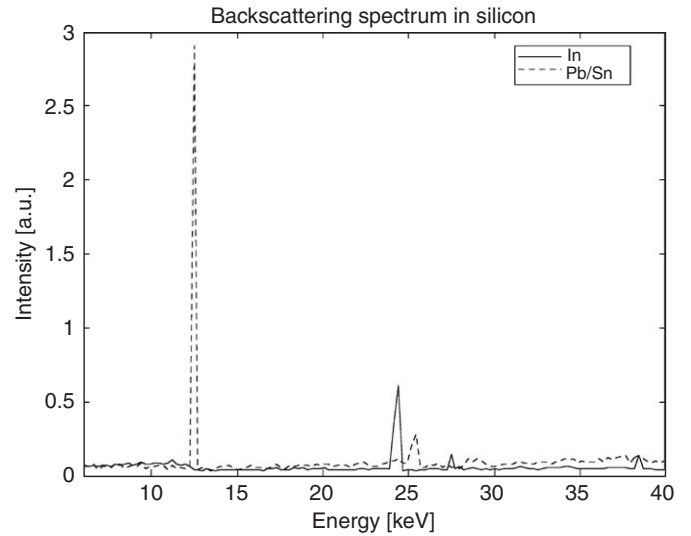


Fig. 3. Spectrum achieved from MCNP due to fluorescence and backscattering from a bump bond consisting of indium or tin/lead. The relative intensity of the 40 keV peak outside the figure is 100.

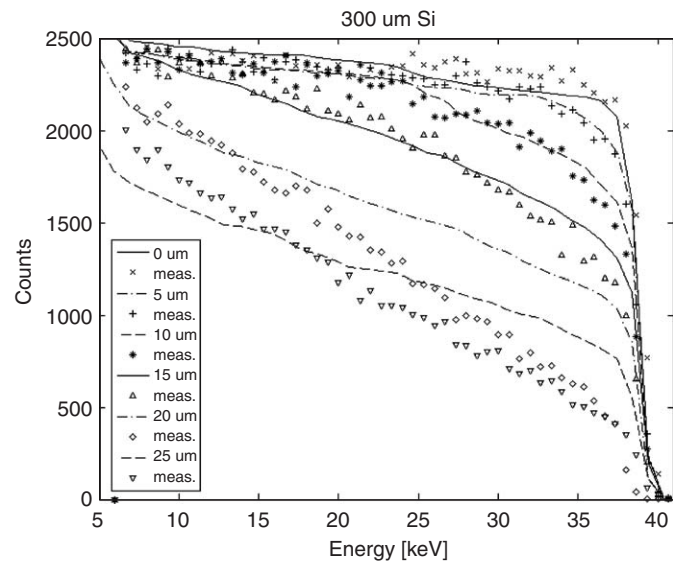


Fig. 4. Comparison of measured and simulated cumulative spectra for a 300  $\mu\text{m}$  thick Si detector. Each spectrum corresponds to a specific beam position relative to the centre of the pixel. The assumed absorbed beam width is 32  $\mu\text{m}$ .

seen as peaks in measurements or simulations, since the fluorescence is radiated spherically and therefore shared between pixels. The fluorescence from the bump-bond is further on referred to as “backscattering”.

2.1. Scanning the beam over the pixel

To be able to see how the charge sharing influences the spectrum, the beam was moved from the centred position towards the border of the pixel. The best spectrum should be achieved with the beam centred above a pixel (0  $\mu\text{m}$ ). The position on the border between two pixels (28  $\mu\text{m}$ ) should give mostly counts from photons with their charge

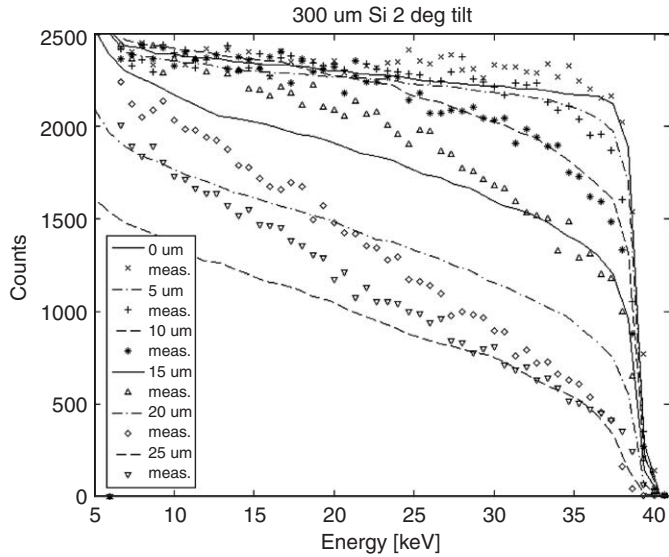


Fig. 5. Comparison of measured and simulated cumulative spectra for a 300  $\mu\text{m}$  thick Si detector. The assumed beam absorption width is 26  $\mu\text{m}$  and the tilt is 2°.

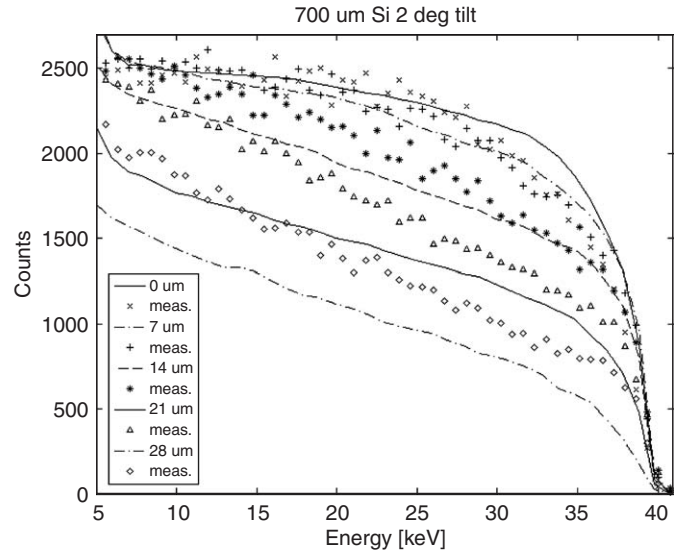


Fig. 7. Comparison of measured and simulated cumulative spectra for a 700  $\mu\text{m}$  thick Si detector. The assumed beam absorption width is 32  $\mu\text{m}$  and the tilt is 2°.

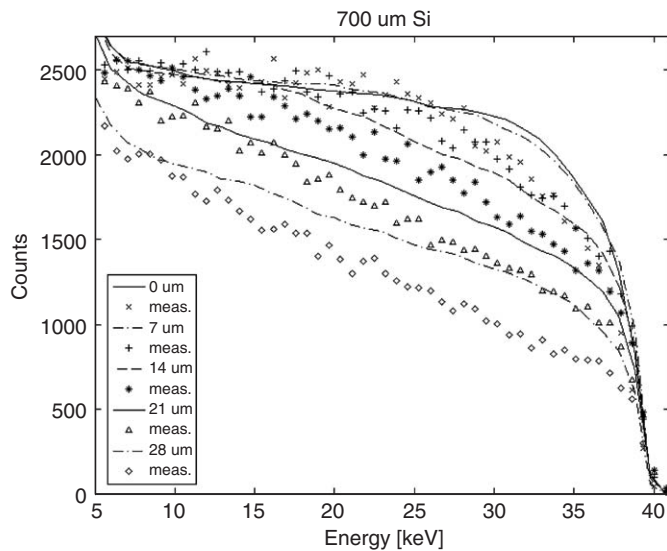


Fig. 6. Comparison of measured and simulated cumulative spectra for a 700  $\mu\text{m}$  thick Si detector. The assumed beam absorption width is 38  $\mu\text{m}$  without tilt.

cloud divided between the two pixels. The resulting cumulative spectra (Fig. 4–7) confirm this behaviour, the slope of the spectra between 10 and 35 keV increases when the beam is moved away from the centred position, indicating that the amount of shared counts increases.

### 3. Simulations

The experimental results have been verified by simulations. The effective beam detected by the readout chip appears to be wider than the actual beam due to scattering and charge drift. If the effective beam is almost as wide as the pixel, charge sharing will take place immediately when

the beam is moved one step from the centre towards the border. On the contrary, for an extremely narrow effective beam only the border position will give an altered spectrum.

Due to X-ray scattering in Si the absorbed beam will be some microns wider than the actual beam, achieved from simulations with MCNP. Charge transport simulations are carried out using a full band self-consistent ensemble Monte Carlo device simulator (GEMS) [7]. A profile of absorbed energy is used as input to the charge transport simulation. The assumptions that are needed to get a reasonable agreement between the measured and the simulated spectra can be used to understand the experimental conditions and the charge sharing process in more detail.

#### 3.1. Simulation of a 300 $\mu\text{m}$ thick Si detector

Simulated spectra for a 300  $\mu\text{m}$  thick detector are compared to measured spectra in Fig. 4. To reproduce the slope of the 40 keV edge in the spectra, a noise level of  $80e^-$  from the readout must be added. This corresponds to the noise expected from the MEDIPIX chip [2] and corresponds to a peak width of approximately 0.7 keV. The contribution of the Fano-factor to the peak width is negligible for silicon. The additional widening of the peak in Fig. 3 and the slight shift to lower energy is due to the charge sharing process. This is indicated by the soft bending at about 38 keV in Fig. 4.

When the energy spectrum of backscattered photons (Fig. 3) is added to the model, the low-energy slope for the centred position will correspond to the measurements. The backscattered photons are assumed to come from a point source located where the beam hits the bump-bond.

To get reasonable position sensitivity for the simulated spectra, the absorbed beam width used in the charge transport simulation must be about  $30\ \mu\text{m}$ . With this beam width the peak width and peak shift in Fig. 3 is also reproduced. This beam width is significantly wider than the absorbed beam width expected from MCNP.

One explanation for the widening of the beam is alignment problems in the setup. The alignment error is assumed to be up to  $2^\circ$  in the direction perpendicular to the axis of the rotation stage. If the beam is tilted, charges created close to the detector surface will reach the readout on a shifted position compared to charges created close to the readout. Charge clouds created close to the surface has a long drift path and will result in wider clouds reaching the readout. A tilted beam will result in more complex position sensitivity for the spectrum. If a  $2^\circ$  tilt is included in the simulations a smaller beam can be assumed and the agreement with measurements is improved (Fig. 5). Note that the peak shift for the border position is reproduced in the simulation when the beam is tilted, but not if the beam is aligned. In the measurements this peak shift is stronger for the  $20\ \mu\text{m}$  position than for the  $25\ \mu\text{m}$  position, indicating an uncertainty in the beam position or imperfections in the detector material.

### 3.2. Simulation of a $700\ \mu\text{m}$ thick Si detector

The comparisons between simulated and measured spectra were carried out for the  $700\ \mu\text{m}$  thick detector also. To reproduce the bended curvature between 30 and 40 keV in the spectra the beam width has to be about  $40\ \mu\text{m}$  without tilt (Fig. 6) and about  $30\ \mu\text{m}$  with  $2^\circ$  tilt (Fig. 7). The agreement is reasonable, but the simulated peak shift for the  $28\ \mu\text{m}$  position in Fig. 7 can not be observed in the measurements. This might be the case if the border position was located about  $10\ \mu\text{m}$  from the border.

The measurement of the  $7\ \mu\text{m}$  position actually shows a more distinct energy edge than the centred position. This indicates a misalignment of the centring for this detector. Simulations show that centring of a tilted beam is a complex problem for the  $700\ \mu\text{m}$  detector. Cases when the  $7\ \mu\text{m}$  position has a higher intensity than the centred position can even occur. The spectrum for the neighbour pixel is also measured (although not shown in the figures). Comparison of these two border positions also indicates a misalignment; since the energy edge of the neighbour is shifted down to 34 keV.

### 3.3. Considerations about simulation accuracy

A uniform absorption depth profile along the beam was assumed in the charge transport simulation. This simplification is valid since silicon is a low absorbing material. The backscattered photons were assumed to be absorbed uniformly in the last  $5\ \mu\text{m}$  of the beam, close the bump bond. This distance was estimated from MCNP simulations were the spherical profile of the backscattered

radiation is verified. The actual range of the radiation is of course much longer in silicon. The absorption profile orthogonal to the beam was assumed to be a uniform square with sharp edges. Test with a soft Gaussian profile gave less agreement with measurements, so it is reasonable to assume that the actual orthogonal absorption profile in fact was sharp. These assumptions about the absorption profile gave a reasonable accuracy to reproduce the conditions of this experiment.

## 4. Conclusions

Position-dependent spectra from a narrow monochrome source at ESRF are achieved with Medipix2 with 300 and  $700\ \mu\text{m}$  thick silicon detectors. It is possible to reproduce the measurements using charge transport simulations and X-ray scattering simulations. The peak width of the simulations fits the measurements if  $80e^-$  readout noise is assumed. Therefore it is likely that the readout noise for the Medipix2 chip is not higher than  $80e^-$  specified in Ref. [2]. The presence of backscattered X-rays from the bump bonds [6] is verified since the low-energy slope of the simulations fits the measurements when backscattering is considered. The size of the absorbed beam was, however, wider than expected from the experimental conditions. It is concluded that the beam must have been tilted in the experimental setup. This angular misalignment has strong influence on the measurements on the  $700\ \mu\text{m}$  thick detector, since it also affects the centring of the beam. An important conclusion is that angular detector alignment will be a problem in the design of high resolution X-ray imaging systems containing thick silicon detectors.

## Acknowledgments

This work was done using detectors, software and readout system developed within the MEDIPIX2 collaboration. The MEDIPIX2-chip is designed at CERN. The MUROS2 readout electronics is designed at NIKHEF and the MEDISOFT4 readout software is developed at University of Napoli.

## References

- [1] B. Mikulec, M. Campbell, E. Heijne, X. Llopart, L. Tlustos, Nucl. Instr. and Meth. A 511 (2003) 282.
- [2] X. Llopart, M. Campbell, R. Dinapoli, D. San Segundo, E. Pernigotti, IEEE Trans Nucl. Sci. NS-49 (2002) 2279.
- [3] K. Mathieson, M.S. Passmore, P. Seller, M.L. Prydderch, V. O'Shea, R.L. Bates, K.M. Smith, M. Rahman, Nucl. Instr. and Meth. A 487 (2002) 113.
- [4] M. Conti, M. Maiorino, G. Mettivier, M.C. Montesi, P. Russo, IEEE Trans Nucl. Sci. NS-50 (2003) 2869.
- [5] J.F. Briesmeister (Ed.), MCNP—A General Monte Carlo N—Particle Transport Code, version 4C, Manual, 2000.
- [6] M. Hoheisel, A. Korn, J. Giersch, Nucl. Instr. and Meth. A 546 (2005) 252.
- [7] H.-E. Nilsson, et al., Nucl. Instr. and Meth. A 487 (2002) 151.